ACS NANO

www.acsnano.org

ARTICLE

# Programmable, Spatiotemporal Control of Colloidal Motion Waves via Structured Light

Xi Chen,[†] Yankai Xu,[†] Kai Lou, Yixin Peng, Chao Zhou, H. P. Zhang,* and Wei Wang*

Cite This: *ACS Nano* 2022, 16, 12755−12766

Read Online

ACCESS | Metrics & More | Article Recommendations | Supporting Information

**ABSTRACT:** **Traveling waves in a reaction-diffusion system are essential for long-range communication in living organisms and inspire biomimetic materials of similar capabilities. One recent example is the traveling motion waves among photochemically oscillating, silver (Ag)-containing colloids. Being able to manipulate these colloidal waves holds the key for potential applications. Here, we have discovered that these motion waves can be confined by light patterns and that the chemical clocks of silver particles are moved forward by reducing local light intensity. Using these discoveries as design principles, we have applied structured light technology for the precise and programmable control of colloidal motion waves, including their origins, propagation directions, paths, shapes, annihilation, frequency, and speeds. We have also used the controlled propagation of colloidal waves to guide chemical messages along a predefined path to activate a population of micromotors located far from the signal. Our demonstrated capabilities in manipulating colloidal waves in space and time offer physical insights on their operation and expand their usefulness in the fundamental study of reaction-diffusion processes. Moreover, our findings inspire biomimetic strategies for the directional transport of mass, energy, and information at micro- or even nanoscales.**

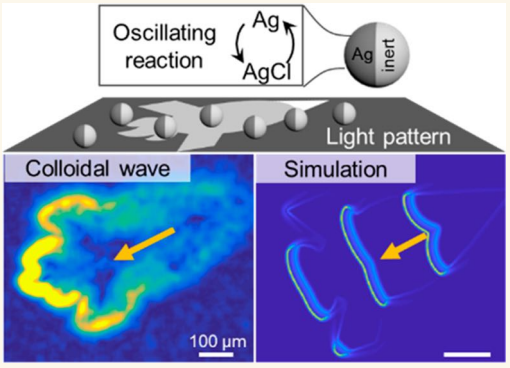


**KEYWORDS:** *chemical wave, active colloids, oscillation, structured light, reaction-diffusion*



Examples of traveling waves are abundant in nature, ranging from self-organizing colonies of microorganisms to physiological processes such as heart beats and neural transmission.[1−4] Chemical waves, in particular, play an important role in regulating and coordinating complex biological functionalities such as the propagation of action potential in the neuron,[5,6] mitotic waves in cell division,[7] and calcium waves in sperm fertilization[8,9] and heart contraction.[10] Synthetic waves arising from oscillating chemical reactions are also plentiful, such as the Belousov−Zhabotinsky (BZ) reaction[11−14] and the oxidation reaction of CO on single-crystal Pt.[15,16] Beyond being a visual wonder, chemical waves could become an essential component in the design of smart materials and devices that autonomously direct the flow of energy, information, and mass over a long distance.[13,17,18]

One way to achieve this goal is to weave the features of traveling waves with micromotors—colloidal particles that autonomously move by converting energy stored in their environment.[19−23] The result is a social microrobot capable of information transmission,[24−26] with far-reaching opportunities as intelligent and reconfigurable materials. On this front, researchers have recently made the intriguing discovery that silver (Ag) microparticles, when exposed to $H_2O_2$, KCl, and light with appropriate wavelengths, oscillate between episodes of fast forward motion and slow diffusion (Figure 1a−c and Video S1).[27,28] This oscillating motion is assumed to be due to a pair of oscillatory reactions on the particle surface:

$$2AgCl + H_2O \xrightarrow{Ag,\ UV\ light} 2Ag + 1/2O_2 + 2H^+ + 2Cl^- \quad (1)$$

$$2Ag + H_2O_2 + 2Cl^- \rightarrow 2AgCl + 2OH^- \quad (2)$$

We proposed recently[29] that the key step in this oscillation cycle is the oxidation of Ag into AgCl (eq 2), which is accelerated by a rising pH from the oxidation itself but suppressed by the photodecomposition of eq 1 that lowers the pH. At a high population density, the oscillating colloids synchronize,[30] giving rise to traveling motion waves in which colloids move back and forth in sequence (see Figure 1d and Video S2 for an example).[27,31] These "swarming waves" typically occur at a period of seconds and travel at hundreds of micrometers per

Received: May 10, 2022
Accepted: July 14, 2022
Published: July 20, 2022




https://doi.org/10.1021/acsnano.2c04596
*ACS Nano* 2022, 16, 12755−12766

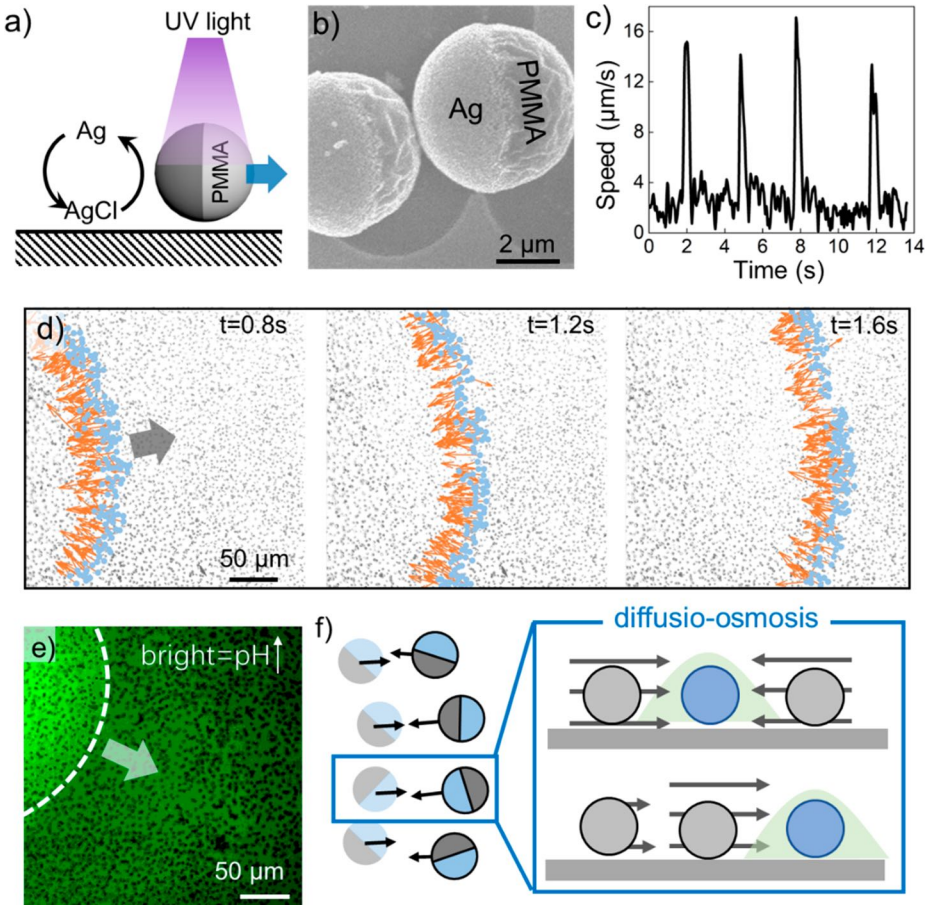


**Figure 1. Oscillating silver colloids and their waves. (a) Chemical oscillation between AgCl and Ag on the surface of a poly(methyl methacrylate) (PMMA) microsphere. (b) Scanning electron micrograph of PMMA-Ag Janus microspheres. (c) Instantaneous speed of a PMMA-Ag microsphere oscillating between episodes of fast and slow motion. Experiments were performed with 0.5 wt % $H_2O_2$, 400 $\mu$m of KCl, and UV light of 500 mW/cm$^2$. (d) Optical micrographs showing the propagation of a colloidal wave. Particles with an instantaneous speed above 6 $\mu$m/s are marked with light blue dots, and their velocity vectors are shown as orange arrows. Experiments were performed with 0.5 wt % $H_2O_2$, 200 $\mu$M KCl, and 100 mW/cm$^2$ UV light intensity and at a 2D particle packing density of 23.0%. (e) Propagation of a fluorescent wave across PMMA-Ag microspheres mixed with a pH-sensitive dye, where brighter fluorescence corresponds to higher pH. Figure adapted under a Creative Commons (CC BY-NC) license from ref 29. Copyright 2022 AAAS. (f) Schematic diagram of a colloidal "swarming wave": a traveling chemical gradient (shown in green shades) sequentially activates colloids (activated spheres are blue), which pulls nearby colloids by diffusio-osmotic flows (gray arrows).**

second. We have recently proposed that colloids in such a "swarming" wave are advected by local osmotic flows generated by a traveling chemical gradient, which is in turn produced by the oscillatory chemical reactions on the particle surface.[29] This speculation was supported by the observation of a propagation $OH^-$ wave (see the fluorescent mapping of local pH in Figure 1e) and qualitatively and quantitatively reproduced by a continuum model that included the reaction and diffusion of activator and inhibitor species (see below for details). Despite this revelation of its operating mechanism, using such colloidal motion waves as an effective strategy to transmit information requires a precise control of the spatiotemporal propagation of waves, which is yet to be accomplished.

Pioneering studies of the spatiotemporal control of BZ waves offer inspiration for controlling colloidal waves. Examples include the use of spatial confinement,[32−35] programmed chemical gradients,[36] electrical potential,[37,38] temperature gradient,[39] audible sound,[40] and light.[41−43] Among these strategies to regulate waves, light confers advantages of spatiotemporal tunability and flexibility. For example, the Showalter group[41] reported a light-controlled feedback method to produce complex wave trajectories in a photosensitive BZ system. Similarly, the Epstein group[44] analyzed the effect of gradient illumination on the traveling direction of waves in BZ gels. Because Ag-containing colloids are similar to BZ systems in that both are sensitive to light (see Table S1 for a more detailed comparison), it is possible to control their waves in spatiotemporally varying light patterns.

We here report the precise and programmable control of colloidal waves in both space and time with structured light technology, building upon two basic design principles that govern where waves start and propagate and their speeds. Carefully designed light patterns generated by structured light then confine traveling colloidal waves to propagate with predetermined origins, paths, directions, and shapes, culminating in waves "drawing" arbitrary shapes such as a rocket or a maze. The temporal control of a colloidal wave, on the other hand, is achieved by a modulation of light intensity that alters the wave speed and frequencies. Finally, we demonstrate the precise control of where and when colloidal waves annihilate. All manipulations are reproduced by a reaction-diffusion model described previously.[29] In the Discussion, we describe how the


https://doi.org/10.1021/acsnano.2c04596
ACS Nano 2022, 16, 12755−12766

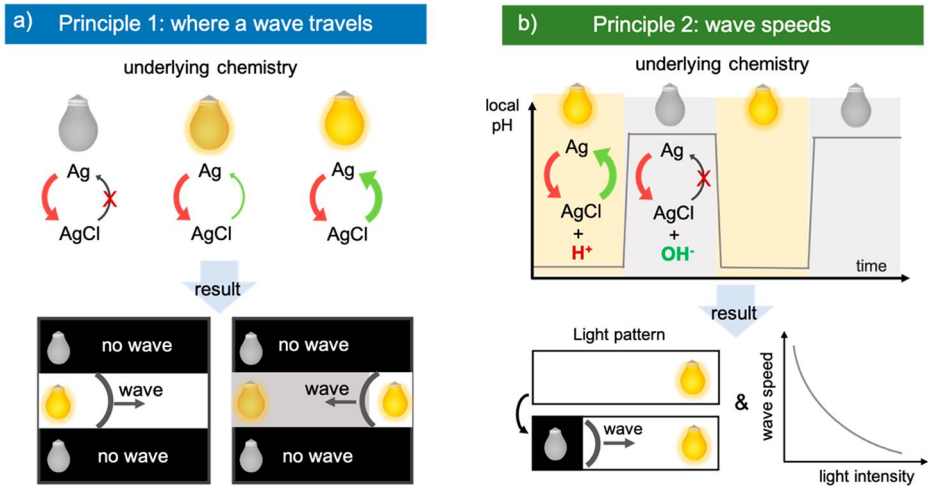


**Figure 2. Design principles for the spatiotemporal control of colloidal waves. (a) Because the decomposition of AgCl into Ag intensifies with increasing light intensity, a colloidal wave is confined in illuminated patches and starts out of the brightest areas. (b) Switching light on and off favors the photodecomposition and oxidation of Ag on the colloidal surface, respectively, which in turn lowers and raises local pH and turns the chemical clock of an oscillating colloid backward and forward, respectively. As a result, waves travel faster in, and initiate out of, dimmed spots. The bottom right plot in part b shows a trend line rather than actual data.**

manipulation of a colloidal wave offers distinct advantages over that of BZ systems and describe future research opportunities in both fundamental and applied fronts. An example is given for information transmission with structured light within a micromotor community.

Overall, our demonstrated capability in the spatiotemporal control of a colloidal wave is useful in clarifying the underlying principles of Ag-containing oscillation, in constructing model systems for studying nonlinear effects, in developing a method of wave-mediated colloidal transport, and in building a biomimetic strategy for the swarm control of communicating micromachines.

## RESULTS

**Design Principles for the Spatiotemporal Control of Colloidal Waves.** Because light is a key ingredient in the oscillation cycle by energizing AgCl to decompose into Ag (eq 1), its spatiotemporal distribution significantly impacts the chemical state of an Ag-containing colloid and, consequently, the propagation of a colloidal wave. This intuition leads to the following two design principles for controlling a colloidal wave in space or time, respectively.

*Principle 1: Where Waves Travel.* Two things can happen when a light pattern is projected on a population of Ag-containing colloids that were originally in the dark. First, only those illuminated can oscillate (Figure 2a, bottom left), because light is essential for converting AgCl back to Ag and, thus, completing the cycle (eq 1). As a result, colloidal waves cannot be sustained in the dark. This principle allows for confining colloidal waves to propagate only in light patterns, with examples given as Figures 3 and 4.

Second, colloidal waves prefer to begin in the brighter regions of a light pattern (Figure 2a, bottom right). This is because AgCl decomposes faster under stronger illumination, which produces more Ag that dials the chemical clock forward to outpace the rest of the particles that are also getting ready. As a result, the brightest spot in a light pattern serves as a pacemaker from which waves propagate, allowing for precisely controlling the origin of colloidal waves. An example is shown in Figure 5.

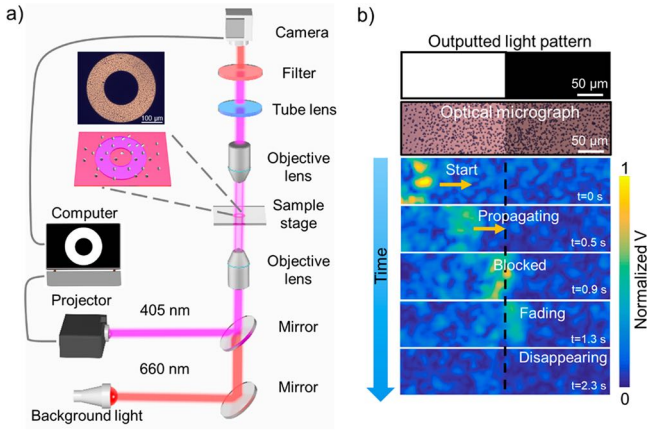


**Figure 3. Confining colloidal waves by structured light. (a) Schematic illustration of an optical setup outputting structured light (see the Experimental Methods for details). (b) Top: Projected pattern that contains an illuminated patch of 200 × 100 $\mu$m at 1660 mW/cm$^2$ next to a dark patch of the same size. Center: The same pattern seen under an optical microscope. In addition to the excitation light, a 660 nm light illumination was used to ensure all particles were visible even in the "dark" patch. Bottom: Flow speeds of a colloidal wave propagating in the light pattern given above. This image was generated by microparticle image velocimetry (micro-PIV), with speeds ranging from blue (slowest) to yellow (fastest). Experiments were performed with 0.5 wt % $H_2O_2$, 200 $\mu$M KCl, and 405 nm light of 1660 mW/cm$^2$ at a 2D particle packing density of 24.8%.**

*Principle 2: Wave Speeds.* Reducing the light intensity of a light pattern, or completely removing light from part of it, slows down the decomposition of AgCl and raises the local pH as a result (Figure 2b.[29] Because, as mentioned earlier and elaborated in ref 29, the oxidation of Ag into AgCl—the key step that excites colloids—is facilitated by a high local pH, a wave is then triggered at the darkening patch (Figure 2b, bottom left) and travels in the rest of the light pattern (shown in Figure 7). For the same reason, a wave also travels faster in darker regions (shown in Figure 8). Note that this operation is only effective when light is reduced on a patch of colloids that have


https://doi.org/10.1021/acsnano.2c04596
ACS Nano 2022, 16, 12755−12766

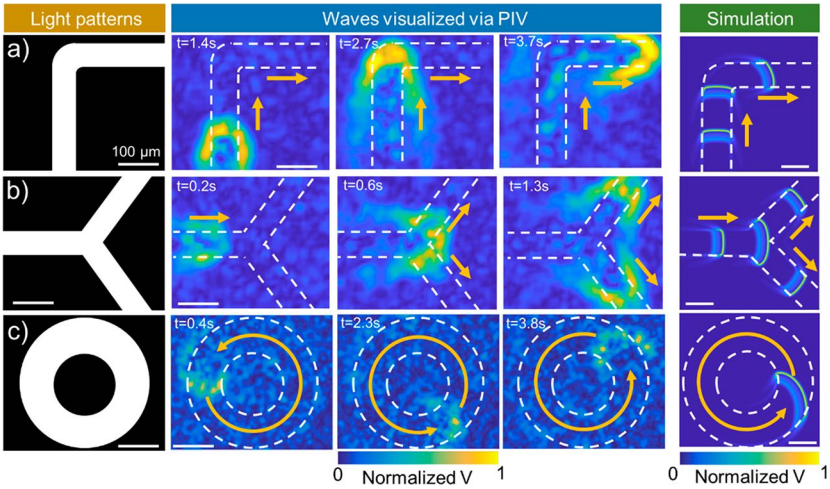


**Figure 4. Guiding colloidal waves in L- (a), Y- (b) and ring-shaped (c) patterns. The left column is the projected light patterns, the middle three columns are PIV images over time, and the rightmost column is the simulated colloids' speeds. All speeds are normalized to their maxima. All scale bars correspond to 100 $\mu$m. All experiments were performed with 0.5 wt % $H_2O_2$, 200 $\mu$M KCl, and 405 nm light of 1660 mW/cm$^2$ at a 2D packing density of 28.7%.**

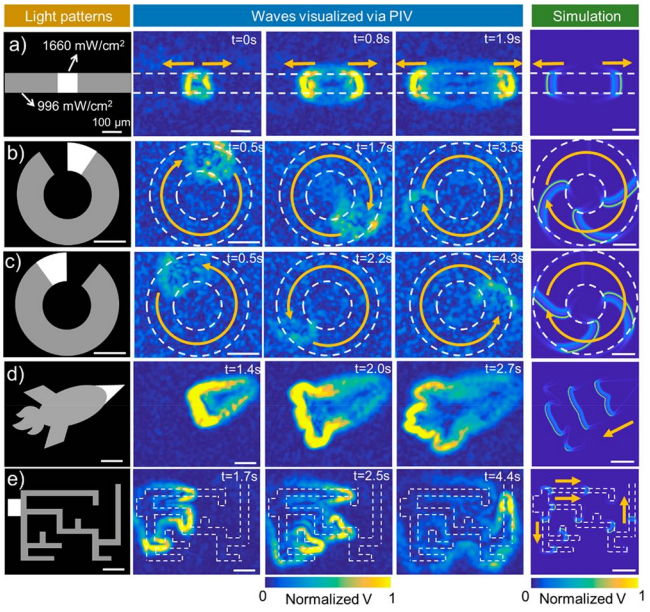


**Figure 5. Complex spatial manipulation of colloidal waves. (a) A wave is initiated at the center of a rectangular pattern where light is brightest and spreads to both ends. (b, c) Colloidal waves are guided to rotate clockwise (b) or counterclockwise (c) in ring-shaped patterns. (d, e) Colloidal waves are initiated at one end and trace the contour of a rocket- (d) or maze-shaped (e) light pattern. The left column is the projected light patterns, the middle three columns are PIV images over time, and the rightmost column is the simulated colloids' speeds. All speeds are normalized to their maxima. All scale bars correspond to 100 $\mu$m. All experiments were performed with 0.5 wt % $H_2O_2$, 200 $\mu$M KCl, and 405 nm light of 1660 mW/cm$^2$ for the brightest regions and 996 mW/cm$^2$ for regions of intermediate brightness. The particles packing density are (a) 22.7%, (b) and c) 17.0%, and (d and e) 13.6%.**

already been illuminated, but not for those that have been in the dark for too long so that the majority of Ag has already converted to AgCl.

**Using Structured Light to Confine Colloidal Waves.** Following Principle 1, we first demonstrate that colloidal waves can be confined in light patterns. This was enabled with a structured light setup that outputs light patterns of arbitrary shapes and sizes with a spatial resolution of 2−3 $\mu$m and a temporal resolution of <0.016 s. The schematic diagram of our structured light setup is shown in Figure 3a, inspired by earlier studies,[45−48] and details are given in the Experimental Methods. The core component is a specialized projector equipped with a digital micromirror device (DMD) that outputs 405 nm (dark purple) light capable of exciting Ag-containing colloids (see Figure S1). Light patterns generated by a computer are then focused through an objective lens onto the sample stage from below so that some colloids receive purple illumination while others remain in the darkness. A red LED lamp (660 nm) incapable of exciting colloids is installed as background lighting so that even colloids not illuminated with purple light can be seen. A CMOS camera collects images through a lens mounted on the other side of the sample stage, with a filter to remove the 405 nm excitation light but not the red background. "Darkness" is then defined throughout this article as a condition with only red but no purple lighting.

To confirm that colloidal waves were able to sense a difference of light intensity, we projected an illuminated rectangular shape of 200 × 100 $\mu$m at 1660 mW/cm$^2$ onto a colloidal population. Typically, poly(methyl methacrylate) (PMMA) microspheres were half-coated with Ag by a vacuum sputterer and suspended in 5 wt % $H_2O_2$ and 400 $\mu$M KCl. Note that the choice of particles was not important, as we have made qualitatively the same observations with Janus microspheres made of polystyrene or silicon dioxide as well as with pure Ag microparticles (see Figure S2). The microparticle image velocimetry (micro-PIV) technique was used throughout this article (except for Figure 1d) to visualize the propagation of waves, where colloids were considered as tracers of fluid flows (see the Experimental Methods for details), and their speeds were marked as colors ranging from blue (slowest) to yellow (fastest). Using micro-PIV, we see in Figure 3b that waves started from one side of the illuminated region and traveled toward the dark region along the long axis of the pattern. At the boundary between the bright and dark regions, the wave front first penetrated into the darkness but then quickly faded and eventually disappeared (Video S3). Additional experiments reveal that whether a wave can penetrate a strip of darkness depends on the strip width and the light


https://doi.org/10.1021/acsnano.2c04596
ACS Nano 2022, 16, 12755−12766

intensity (Figure S3). These combined results confirm that waves can be confined to only propagate in illuminated areas, in accordance with Principle 1.

**Manipulating Colloidal Waves in Space.** Having established that light patterns can confine propagation of waves, we further regulate waves in more complex virtual confinements, drawing inspiration from earlier studies of the interplay between the confinement geometry and wave dynamics in reaction-diffusion systems.[32,49−51] Notably, all wave dynamics and manipulations reported in this section can be reproduced with a numerical model based on reaction-diffusion principles (see the Supporting Information (SI) and ref 29 for details). Briefly, this model was built upon the Rogers−McCulloch model,[52] widely used for modeling the reaction-diffusion process, and considers the generation, consumption, and diffusion of an activator and an inhibitor species. The nonlinear interplay between their concentrations then gives rise to chemical waves. Note that quantitative comparison between the model and experiments, including the exact shapes and speeds of waves, is challenging, because our phenomenological model does not contain exact chemical details and it is a continuum model whereas experiments contain discrete particles. Nevertheless, the qualitative agreement between the two suggests that colloidal waves are underpinned by a traveling chemical gradient, echoing our earlier study.[29]

We describe below the various ways colloidal waves can be regulated in space. First, colloidal waves can sense the geometry of spatial light patterns, which lays the foundation for subsequent manipulation of waves in complex light patterns. For example, colloidal waves preferred to begin at the corners in triangular, rectangular, or pentagonal confinements (Figure S4), consistent with waves traveling in BZ gels.[51] This preference to start at a corner is likely caused by the higher concentration of $H_2O_2$, and thus more activators, at a corner where chemicals can diffuse in from more directions than the rest of the pattern. The choice of at which corner to start is, however, stochastic and possibly related to the random fluctuation of particle number density (Figure S4). It is, therefore, possible for waves to emerge out of two corners simultaneously (Figure S5). Moreover, waves tended to travel parallel to the long axis of a light pattern of low aspect ratios and along the diagonal of rectangular patterns of high aspect ratios (Figure S6).

Using this knowledge, we guided waves along the predefined paths in Y-, L-, and ring-shaped patterns (Figure 4 and Video S4). When reaching the corner of an L-shaped pattern (Figure 4a), a colloidal wave did not persist in the original direction (and into the darkness) but rather turned and traveled along the pattern. When propagating in a Y-shaped pattern, on the other hand, a wave split at the intersection and continued to travel along both branches (Figure 4b). Finally, waves in a ring-shaped pattern (Figure 4c) started from random locations and fused and annihilated with each other over time, eventually rotating persistently around the ring-shaped pattern either clockwise or counterclockwise. Its handedness can be further controlled using techniques shown in Figure 5b and c.

Next, we show how to control the origin of a colloidal wave according to Principle 1. Earlier studies have shown that individual micromotors oscillate more intensely under stronger illumination,[28] possibly because of a faster photodecomposition of AgCl that quickly builds up Ag that subsequently reacts with $H_2O_2$ to induce propulsion. This knowledge, summarized into Principle 1, leads to the design of a small patch of "pacemaker" colloids, similar to the cardiac pacemaker cells that control the heart rate, by exposing them to a much stronger illumination than their neighbors. As a result, the surfaces of the "pacemaker" colloids are quickly converted to Ag and enter the excited state earlier than the rest of the colloids. Experimentally, we projected a rectangular pattern with a small patch in the middle that is significantly brighter than the rest of the pattern (1660 vs 996 mW/cm$^2$). A wave indeed started at the bright patch and spread to the ends, shown in Figure 5a and Video S5a. The fact that waves prefer to begin at bright spots further enables the control of the chirality of propagating waves, as shown in Figure 5b and c (Video S5b and c).

The above knowledge of how waves can be confined, split, be initiated, and make turns lead to the capability of manipulating colloidal waves in complex light patterns. For example, waves propagate from the nose to the tail of a cartoon rocket while sketching out its contour in Figure 5d and Video S5d, by projecting a light pattern of a cartoon rocket with a bright nose. Moreover, a traveling wave in Figure 5e and Video S5e explored the entire maze and found its exit, taking advantage of the facts that (i) a wave always travels along the long axis of a maze branch, (ii) it always splits into multiple waves at intersections, and (iii) it disappears at a dead end. These results of wave propagation along complex geometries suggest the potential use of colloidal waves in long-distance information transmission in tortuous, heterogeneous, or highly porous environments.

The shape of a colloidal wave can also be regulated. A wave front in a reaction-diffusion system typically propagates outward either in concentric circles or in spirals, termed target waves or spiral waves, respectively.[53] Both types of waves are common for populations of Ag-containing colloids,[29] but it has been difficult to select one over the other. By projecting a ring-shaped light pattern with a bright spot at the center (Figure 6a and Video S6a), sustained target waves are generated in a way similar to the construction of "pacemakers" described above (i.e., Figure 5).

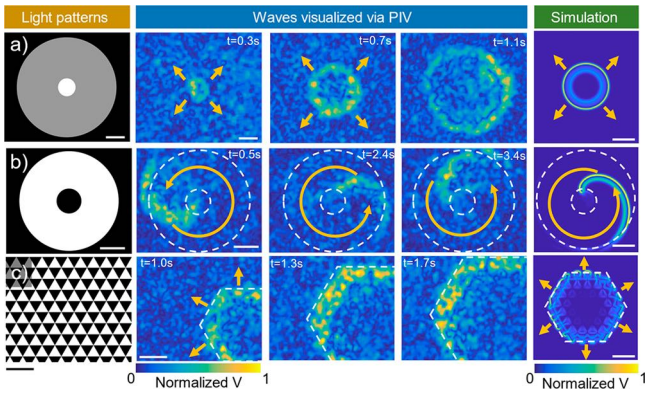


**Figure 6. Tuning of the shapes of colloidal waves. (a) Target waves are initiated from a bright spot in a circular light pattern. (b) Spiral waves are pinned to a dark core and rotate in a ring-shaped light pattern. (c) Hexagonal wave fronts propagate in a checkerboard pattern filled with triangular cells alternating spatially between brightness and darkness. The left column is the projected light patterns, the middle three columns are PIV images over time, and the rightmost column is the simulated colloids' speeds. All speeds are normalized to their maxima. All scale bars correspond to 100 $\mu$m. All experiments were performed with 0.5 wt % $H_2O_2$, 200 $\mu$M KCl, 1660 mW/cm$^2$ 405 nm light in the brightest regions, and 996 mW/cm$^2$ light in the intermediate regions. The particle packing densities were 10.8%, 16.9%, and 14.8% for parts a, b, and c, respectively.**



https://doi.org/10.1021/acsnano.2c04596
ACS Nano 2022, 16, 12755−12766

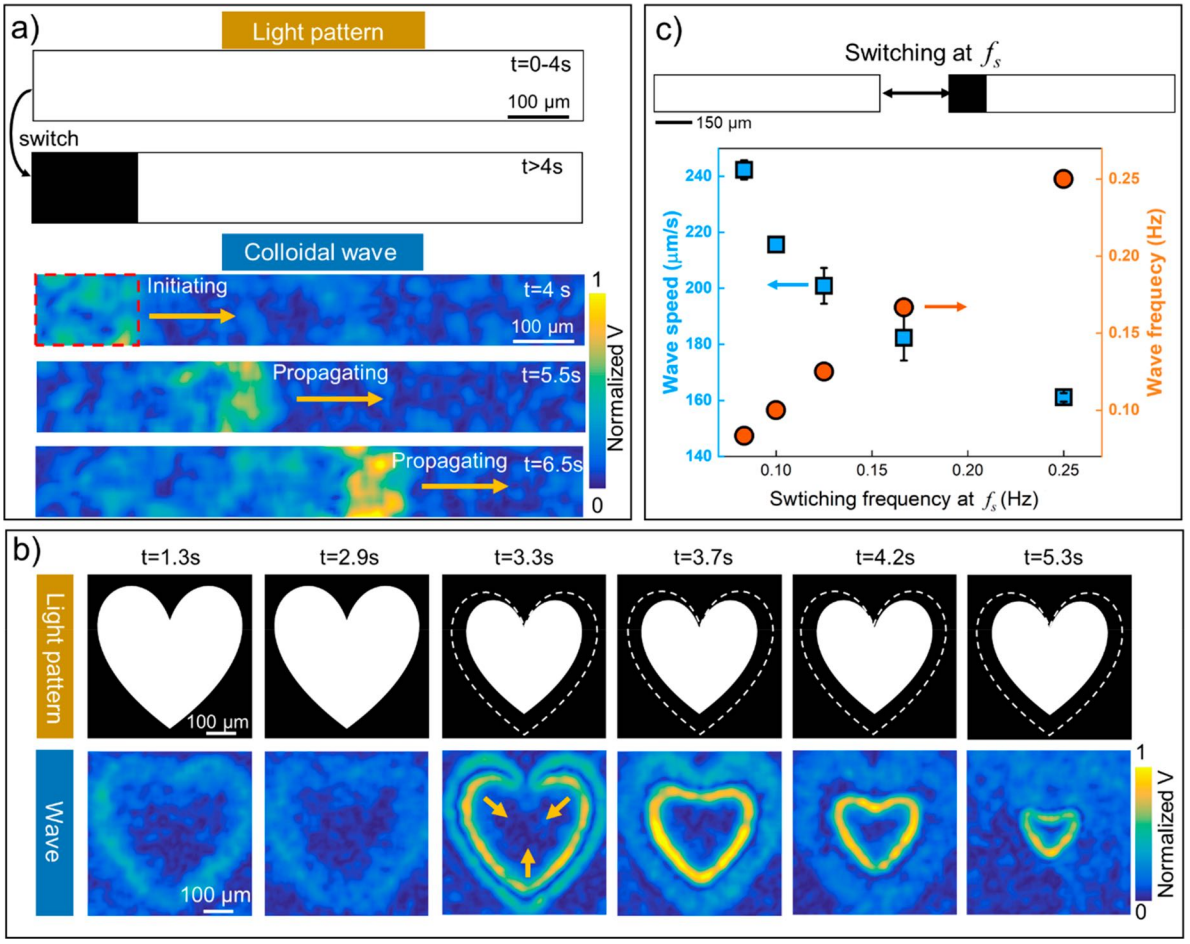


**Figure 7. Temporal manipulation of colloidal waves. (a) Top: Schematic of switching off the light for a 150 $\mu$m × 225 $\mu$m segment in a 150 $\mu$m × 880 $\mu$m light pattern. Bottom: PIV images of the resulting colloidal wave. (b) A colloidal wave is initiated at the darkness−brightness boundary of a heart-shaped light pattern and propagates into the brightness. (c) Top: Schematic of periodically switching the light on and off for a 150 × 150 $\mu$m square located at one end of a long bright pattern. Bottom: Speeds and frequencies of the resulting colloidal waves at different switching frequencies $f_s$. Experiments were performed with 0.5 wt % $H_2O_2$, 200 $\mu$M KCl, and 405 nm light of 1660 mW/cm$^2$ at particle packing densities of (a) 10.9% and (b) 18.1%.**

Sustained spiral waves, on the other hand, are generated in a ring-shaped light pattern with a *dark* spot at its center (Figure 6b and Video S6b). As a common principle for generating spiral waves,[54] this dark spot breaks the propagation of a reaction-diffusion wave so that a spiral wave is pinned to the dark core and rotates in the ring.

The last piece in our toolbox for the spatial manipulation of colloidal waves is shaping wave fronts beyond the typical arcs. To do so, we projected a checkerboard light pattern filled with triangular cells of alternating brightness (Figure 6c and Video S6c). Because waves can transmit across small barriers but not large ones (see Figure S3), dark cells above a certain size cut off the local wave propagation so that it can only propagate in the illuminated cells, leading to a wave front of a hexagonal shape. Similar results have been reported in BZ systems.[33]

**Manipulating Colloidal Waves in Time: Wave Speeds and Frequency.** In addition to controlling how a colloidal wave propagates in space, it is equally important to tune its dynamics in time, such as its speed and frequency. For this purpose, the intensity of the light is varied in time rather than space, following Principle 2. This operation is inspired by our recent discovery that Ag-containing oscillating colloids exhibit a singular dash upon switching off the light, an observation we termed "dark pulse".[55] Further studies[29] have suggested that switching the light off raises the solution pH, which triggers a wave.

As a result, projecting a dark spot on an illuminated background to raise the local pH can trigger a wave at that spot that propagates outward. This is tested by first projecting a light pattern of 150 $\mu$m × 880 $\mu$m onto a population of Ag colloids for 4 s (Figure 7a) and then turning off the light only for a 150 $\mu$m × 225 $\mu$m area at one end of the pattern. Indeed, a wave was initiated from the dark spot and propagated along the rest of the pattern that remained illuminated (Video S7). A closer look suggests that these waves initiated by dark spots follow the boundary contour between the bright and dark sections and always move from the dark to the bright side. This is demonstrated in Figure 7b and Video S8, where a heart-shaped wave is generated by shrinking a heart-shaped light pattern, which is equivalent to turning off the light for colloids lining the pattern's edge.

Because a wave is generated once the light is turned off, turning it on and off periodically then produces periodic waves with frequencies entrained to the switching frequency $f_s$. For example, we periodically switched the light on and off for a square of 150 × 150 $\mu$m located at one end of a long rectangular pattern that was constantly lit (Figure 7c). The frequencies of the resulting wave were entrained to the switching light ($f_s$) for


https://doi.org/10.1021/acsnano.2c04596
ACS Nano 2022, 16, 12755−12766

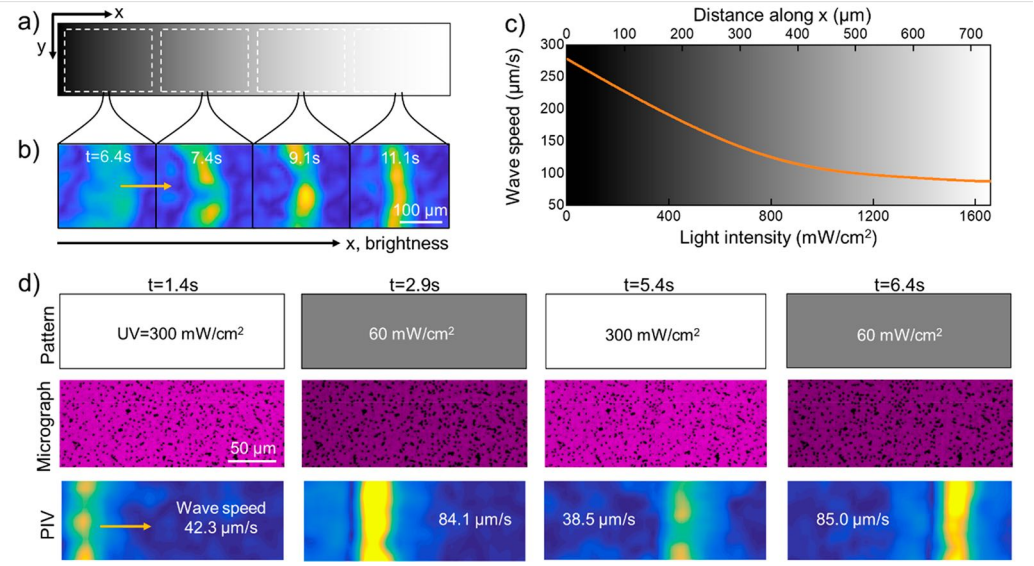


**Figure 8. Tuning wave speeds *in situ*.** (a–c) Tuning wave speeds by modulating light in space (Video S10a). (a) Schematic of a gradient light pattern of 734 × 200 $\mu$m, which was applied 6 s after the same area had been illuminated uniformly. (b) PIV images of the resulting colloidal wave moving from left to right along the pattern. (c) Wave speeds at different positions (and thus different light intensities) in the case sof parts a and b. (d) Tuning wave speeds by modulating light over time (Video S10b). Waves accelerate on the fly when decreasing the light intensity of the entire field of view ($t$ = 2.9 and 6.4 s) and decelerate when increasing light intensity ($t$ = 1.4 and 5.4 s). Experiments were performed with 0.5 wt % $H_2O_2$, 200 $\mu$M KCl, and (b) 405 nm light at a particle packing fraction of 24.2% and (d) 365 nm light at a particle packing fraction of 11.9%.

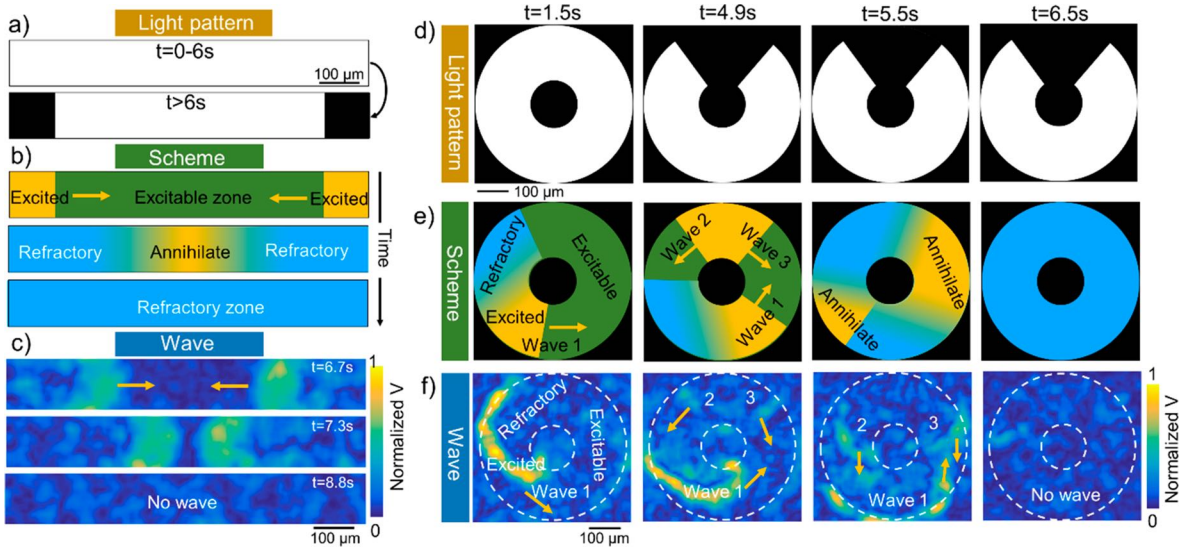


**Figure 9. Controlled annihilation of colloidal waves.** (a–c) Turning off light at both ends of a rectangular light pattern excites two colloidal waves that move toward each other. They both disappear after colliding, because they are unable to propagate in each other's refractory zones. (d–f) Turning off light at a segment in a ring-shaped pattern produces two waves (waves 2 and 3) that propagate in opposite directions around the ring, terminating the existing wave 1. All scale bars correspond to 100 $\mu$m. Experiments were performed with 0.5 wt % $H_2O_2$, 200 $\mu$M KCl, and 405 nm light of 1660 mW/cm$^2$ at particle packing densities of (c) 23.8% and (f) 28.7%.

$0.08 \leq f_s \leq 0.25$ Hz. The lower limit of 0.08 Hz corresponds to the intrinsic frequency of a wave (i.e., a period of ~12.5 s), below which the wait before switching light was too long and waves had already started spontaneously. Switching light on and off at a frequency $f_s$ larger than 0.25 Hz, on the other hand, was too fast for waves to begin, presumably because of too little activator and/or too much inhibitor to trigger a wave. How these threshold frequencies, which are case specific, are linked to the chemical kinetics of the oscillatory reactions is an interesting subject that remains to be explored.

Wave speed is a critical component in the temporal modulation of colloidal waves, and it can be tuned in two ways. First, as Figure 7c suggests, wave speeds decrease with increasing $f_s$, known as a dispersion relation common to a reaction-diffusion system.[56] To qualitatively understand why waves travel more slowly at high $f_s$, we speculate that neither the photodecomposition of AgCl to Ag nor its oxidation back to AgCl can react fully when light is switched on and off frequently (i.e., at a high $f_s$), so that waves are, therefore, forced to propagate in a medium that is still recovering, which slows down a wave.



https://doi.org/10.1021/acsnano.2c04596
ACS Nano 2022, 16, 12755–12766

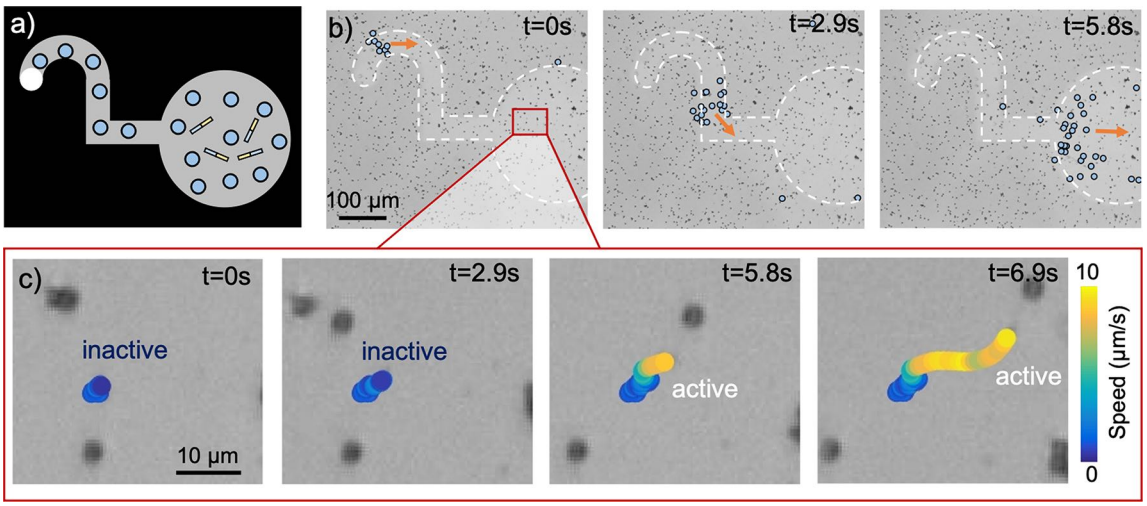


**Figure 10. Controlled activation of bimetallic microrods by chemical waves confined in a light pattern. (a) Schematic of the light pattern and the locations of silver particles (blue dots) and microrods. The brightest spot at the top-left corner of the pattern is the starting point of the signal. Objects are not drawn to scale. Inset: SEM image of a Au−Rh bimetallic microrod. (b) Optical micrographs of a mixed colloidal population overlaid with the locations of the wave fronts at different time instances. Activated silver particles (speed >5 $\mu$m/s) are labeled light blue, and the wave direction is labeled with an arrow. (c) Enlarged view of the section of the light pattern labeled in part b at different time instances. These micrographs are overlaid with the trajectory of one microrod, color-coded with its instantaneous speeds. In this experiment, gold−rhodium microrods of ∼2−3 $\mu$m long and ∼200 nm diameter were mixed with PMMA-Ag Janus microspheres of 2.5 $\mu$m diameter. They were suspended in 0.5 wt. % $H_2O_2$ and 200 $\mu$M KCl and illuminated with 405 nm light of 996 mW/cm$^2$ (the light intensity is 1660 mW/cm$^2$ at the brightest spot).**

Alternatively, wave speed can be varied *on the fly* by modulating light intensity in space or time (Figure 8 and Video S9). For example, Figure 8a−c shows that a wave travels faster in the darker regions in a gradient of illumination intensity, consistent with Principle 2. In principle, light gradients more complex than Figure 8a can be designed so wave speeds change nonmonotonically in the course of propagation. Furthermore, instead of varying light intensity spatially, it can also be varied temporally as a wave propagates. The results in Figure 8d show how a wave moves faster when light is dimmed and more slowly when light is turned brighter as it travels to the right. Finally, the variation of wave speeds with light intensity allows for terminating a wave at an arbitrary position, by increasing the light intensity of a particular spot in a light pattern so that waves converge and terminate at this brightest spot of the lowest wave speed (Figure S7 and Video S10).

**Manipulating Colloidal Waves in Both Space and Time.** Combining the above capabilities, we demonstrate below the annihilation of multiple waves, in which colloidal waves are controlled in *both* space and time.

In an early study,[29] we have seen that two colloidal waves upon colliding do not go through each other and continue but rather annihilate and disappear. This is because of an excess of inhibitors behind a colloidal wave, so that colloidal particles need time to recover (known as the "refractory period"). Such annihilation among reaction-diffusion waves is a common phenomenon,[57,58] yet it typically occurs at random places and times for colloidal waves. However, by controlling where and when colloidal waves are triggered, we can precisely set when and where they annihilate. This is demonstrated in Figure 9a by turning off light at both ends of a rectangular pattern, so that two waves were initiated and headed toward each other and finally annihilated and disappeared at the middle of the light pattern (Figure 9b and c and Video S11a). As expected, the waves moved toward but not through each other.

The same principle of wave annihilation can also be applied to ring-shaped light patterns, which as we described in Figure 6b spawned spiral waves of random handedness ("wave 1" in Figure 9d). As Figure 9d depicts, we then switched off the light on a small patch on the top of the ring pattern, triggering two waves that propagated in opposite directions around the ring (waves 2 and 3). Wave 3 then collided with and annihilated the original wave 1 in the same way as Figure 9a−c, while wave 2 caught up with the refractory tail of wave 1 and terminated. In the end, the entire ring pattern is wavefree. This process is described in Figure 9e and f and shown in Video S11b. Interestingly, the same principle has been used in the treatment of cardiac arrhythmias by eliminating unwanted spiral waves propagating among cardiac cells.[59]

## DISCUSSION

**Manipulating Colloidal Waves vs BZ Waves.** Although sharing the same scientific and technological principles, the spatiotemporal manipulation of a colloidal wave offers distinct advantages over that of classical BZ patterns (their similarities and differences are summarized in Table S1). First and foremost, a classical BZ system does not contain colloidal particles that produce and respond to traveling chemical waves. As a result, mass transport within BZ systems occurs either at molecular scales for chemicals constituting an oscillatory reaction network or at a macroscopic scale for droplets[60] or gels.[61] A colloidal wave, on the other hand, occurs at an intermediated scale with discrete, visible entities. Moreover, most studies of manipulating BZ patterns have focused on their propagation in space,[49,51,62] whereas we have achieved both spatial and temporal control of colloidal waves by taking advantage of their response to switching the light off.

**Future Prospects for Controlling Colloidal Waves.** The demonstrated capability in manipulating a colloidal wave can be extended in three directions. First, oscillating colloids could spontaneously form patterns upon switching light on and off, drawing inspiration from reports that a rotating spiral wave in a BZ system can transform into a labyrinthine standing-wave pattern when light is toggled at specific frequencies.[63] Second,


https://doi.org/10.1021/acsnano.2c04596
ACS Nano 2022, 16, 12755−12766

dynamic light patterns that vary in space and time could enable the dynamic manipulation of oscillating colloids, as showcased in recent examples of nonoscillating active colloids.[64,65] For example, it is possible to unpin and move a spiral wave such as that in Figure 6b to a specific location by moving the dark core. Finally, a feedback-regulated light gradient could enable real-time control in the trajectory and geometry of waves.

**Usefulness of Controlling Colloidal Waves.** The spatiotemporal control of a colloidal wave could have exciting possibilities in both fundamental and applied areas. For the fundamental study of nonlinear sciences, photochemically oscillating colloids are emerging as a reliable and adjustable model system of reaction-diffusion processes, as a number of studies over the past decade have revealed.[27−31,55,66,67] The capability of precisely tuning their dynamics in space and time further allows for testing existing theories and discovering potential research opportunities. For example, the interplay between self-motile colloidal particles[22,68] with chemical waves could give rise to exotic phenomena such as swarm oscillators[69] or hierarchic self-organization[70,71] mimicking social amoeba.[72] These interesting questions would not be possible to probe with classical BZ systems because of a lack of mesoscopic agents that are visible, are tunable, and move autonomously.

For applications, by regulating when and where a colloidal wave travels, it is possible to transport colloidal matter in a contactless and directional manner,[17,61,73] including syntenic nano- and microparticles, bacteria, or even cells, especially when integrated with other existing techniques such as acoustic tweezers,[74] optical tweezers,[75] or microfluidics. For example, one can imagine a practical scenario where functional colloidal particles are transported on a microchip along a predefined, yet erasable, path generated by structured light and then assemble at target areas as biosensors or pillars for sorting. Although similar transport of colloidal matter has been reported using traveling light pulses,[65] or propagating waves of nanosheets[76] or nanofibers,[17] none have achieved the same level of spatiotemporal control demonstrated in this report. More effort is needed to confirm that such mesoscopic transport can be harnessed to do useful work.

In addition, there is a pressing need for coordinating a group of autonomously moving micro-/nanorobots in a complex environment such as human bodies.[77,78] A key requirement in this application is fast information relay through a large group of microrobots, without distortion, and preferably along a winding, branched path. Recent studies have demonstrated how information can be relayed among microrobots through hydrodynamic interactions[79] or chemical signals.[25,80] The colloidal wave studied here is another biomimetic strategy to achieve this goal,[30] by illuminating *in vivo* a microrobot swarm with programmable structured light that adapts to a changing environment, possibly by flexible optical fibers.[81,82] Figure 10 and Video S12 demonstrate a very preliminary example. Previously, we have discovered that the chemicals released by an oscillating silver particle can activate nonoscillatory bimetallic microrods into a pulse of directional motion.[67] Here, silver microparticles were randomly scattered in the entire field of view, and a chemical wave traveled in a light pattern toward a wide opening, where a small population of bimetallic microrods were located. These rods remained Brownian until the chemical wave reached them, upon which they began to move autonomously and ballistically. Although this demonstration is quite simple, the start and finishing points, the path, and the speed and frequency of such an activation event can, in principle, be precisely controlled following the principles detailed above.

## CONCLUSION

In summary, we have proposed two design principles to precisely manipulate colloidal waves traveling across a population of photochemically activated, Ag-containing colloids in both space and time. These principles are intricately related to how the oscillation between Ag and AgCl adjusts and responds to local pH and how only half of the cycle is light-sensitive. As a result, waves sense differences in illumination intensity and are, therefore, confined in spatial light patterns generated by structured light, enabling the precise and programmable control in their origins, paths, directionality, and shapes. The temporal modulation of colloidal waves is achieved by modulating light intensity, which determines not only when and where a wave is triggered but also its speed and frequency. Looking forward, the spatiotemporal control of colloidal waves not only expands their usefulness in the fundamental study of reaction-diffusion processes but also inspires biomimetic strategies for the directional transport of mass, energy, and information at micro- or even nanoscales.

## EXPERIMENTAL METHODS

**Sample Fabrication.** Colloidal self-assembly at a liquid−liquid interface was used to prepare a monolayer of poly(methylmethacrylate) (PMMA) microspheres. Specifically, 3 mL of hexane was added to the surface of 20 mL of water to form a water−hexane interface. Then, 50 $\mu$L of 5% PMMA microspheres suspended in ethanol was prepared. The suspension was added dropwise onto the water−hexane interface so that the PMMA microspheres self-assembled into a monolayer, which was then transferred onto a piece of Si wafer. Janus PMMA-Ag microspheres were fabricated by evaporating a 50 nm layer of Ag onto the monolayer of PMMA microspheres via electron beam evaporation (TF500, HHV). Gold−rhodium microrods were synthesized by electrodeposition in an alumina oxide template, following ref 67.

**Colloidal Wave Experiments.** An inverted optical microscope (Olympus IX71) was used to observe the motion of Janus PMMA-Ag particles under uniform illumination. A LED UV lamp (Thorlabs M365LP1-C1, central wavelength at 365 nm) excited Janus colloids from above. A ring-shaped white LED lamp that is incapable of exciting colloids was placed around the UV lamp to provide background illumination for imaging. In a typical colloidal wave experiment, PMMA-Ag colloids were suspended in 0.05 wt. % $H_2O_2$ and 200 $\mu$M KCl, and the resulting suspension was pipetted into a homemade chamber. After few minutes, the majority of PMMA-Ag colloids settled down on the glass substrate with a particle packing density over 10%.

**Structured Light.** A schematic is given in Figure 3a. The core component of this setup is a specialized projector (SM7-405, SICUBE) containing a digital micromirror device (DMD) to project light patterns. It outputs 405 nm light (maximum light intensity is 9.4 W/cm$^2$) that is capable of exciting Janus PMMA-Ag colloidal particles. Light patterns are then focused through an objective lens onto the sample stage from below so that some colloids receive purple illumination while others remain in darkness. In addition, a LED lamp (Thorlabs M660L4) that outputs 660 nm light incapable of exciting particles was used to provide background illumination for imaging (see Figure S1 for confirmation). "Darkness" is defined throughout this article as a condition with only 660 nm but no 405 nm illumination. A CMOS camera (GS3-U3-51S5C-C, Point Gray) collected images through an objective lens and a tube lens mounted on the other side of the sample stage, with a bandpass filter that removes the 405 nm excitation light but allows for the 660 nm illumination. Videos were recorded typically at 15 frames per second. A computer was connected with the projector to create light patterns of different sizes and shapes generated by Microsoft PowerPoint. The light


https://doi.org/10.1021/acsnano.2c04596
ACS Nano 2022, 16, 12755−12766

intensity can be modulated by a custom computer program or adjusting the RGB intensity of the pictures in PowerPoint.

**Single-Particle Tracking and Visualization of Colloidal Waves.** The xy coordinates of the colloidal particles were extracted by homemade MATLAB codes to obtain their trajectories and instantaneous speeds. Two methods were used to visualize the propagation of colloidal waves. The first one was to mark colloids whose speed exceeded a threshold (6 $\mu$m/s) with light blue dots and orange arrows overlapping the original optical micrograph (e.g., Figure 1d in the main text). This was done with homemade MATLAB code. The second method was to apply microparticle image velocimetry (micro-PIV). Micro-PIV is commonly used to map the fluid velocity field by calculating the displacement of tracer microparticles distributed in the flow field. In a typical procedure, a video was decomposed into image sequences and imported into Fluere, a free software to calculate the displacement of microparticles between images to yield the instantaneous velocity field. In our case, speed data at each node point ($65 \times 65$ pixels in a $2048 \times 2048$ pixel image) was calculated and a new video was generated with velocities coded in colors.

**Numerical Simulation.** A Rogers–McCulloch model[52] that has been widely used to describe waves in reaction-diffusion systems was used to reproduce wave behaviors in experiment, following ref 29. See the SI for the details of its implementation. This model involves two key variables: the concentration of an activator species (termed $u$) that promotes the chemical reaction and that of an inhibitor (termed $v$) that suppresses the reaction. The spatiotemporal interplay of $u$ and $v$ leads to chemical waves. Based on the assumption that colloids trace a neutral osmotic flow caused by a chemical gradient, the gradient profile $\nabla u$ in the simulation can then be related to the actual colloids velocity $V$ profile in the experiment via $V \propto \nabla u$.[29] As a result, we can map out the colloidal wave in simulation. To simulate the propagation of waves in a light pattern, the activator is assumed to be able to both react and diffuse in the bright region but only able to diffuse in the dark region. To simulate the wave in light patterns with different light intensities, initial values of $u$ and $v$ are set to be 1 and 0, respectively, in the brightest region.

## ASSOCIATED CONTENT

### Supporting Information

The Supporting Information is available free of charge at https://pubs.acs.org/doi/10.1021/acsnano.2c04596.

Details on numerical simulation, single-particle dynamics in light patterns (Figure S1), waves out of $SiO_2$–Ag and pure Ag particles (Figure S2), additional figures of waves in different light patterns (Figures S3–S7), and a comparison between colloidal waves and BZ waves (Table S1) (PDF)

Video S1: Typical dynamics of an oscillating micromotor (MP4)

Video S2: Representative colloidal wave traveling across a population of PMMA-Ag colloids and propagation of a chemical wave in the reaction-diffusion model (MP4)

Video S3: Colloidal wave traveling along the illuminated area and stopping at the interface between the illuminated and dark areas (MP4)

Video S4: Colloidal wave propagating along predefined paths in Y-shaped, L-shaped, and ring-shaped patterns (MP4)

Video S5: Complex spatial manipulation of colloidal waves and corresponding simulation results (MP4)

Video S6: Controlling the shape of colloidal waves and corresponding simulation results (MP4)

Video S7: Controlling when and where a colloidal wave begins by turning off light locally (MP4)

Video S8: Controlling the shape of colloidal waves by turning off light locally (MP4)

Video S9: Tuning wave speeds *in situ* (MP4)

Video S10: Guiding colloidal waves to converge to specific spots (MP4)

Video S11: Controlled annihilation of colloidal waves (MP4)

Video S12: Controlled activation of a micromotor of bimetallic rods by chemical waves confined in a light pattern (MP4)

## AUTHOR INFORMATION


### Corresponding Authors

**H. P. Zhang** – *School of Physics and Astronomy and Institute of Natural Sciences, Shanghai Jiao Tong University, Shanghai 200240, China*; Email: hepeng_zhang@sjtu.edu.cn

**Wei Wang** – *Sauvage Laboratory for Smart Materials, School of Materials Science and Engineering, Harbin Institute of Technology (Shenzhen), Shenzhen 518055, China*; orcid.org/0000-0003-4163-3173; Email: weiwangsz@hit.edu.cn

### Authors

**Xi Chen** – *Sauvage Laboratory for Smart Materials, School of Materials Science and Engineering, Harbin Institute of Technology (Shenzhen), Shenzhen 518055, China*

**Yankai Xu** – *School of Physics and Astronomy and Institute of Natural Sciences, Shanghai Jiao Tong University, Shanghai 200240, China*

**Kai Lou** – *Guangzhou Kayja-Optics Technology Co., Ltd., Guangzhou 511458, China*

**Yixin Peng** – *Sauvage Laboratory for Smart Materials, School of Materials Science and Engineering, Harbin Institute of Technology (Shenzhen), Shenzhen 518055, China*

**Chao Zhou** – *Sauvage Laboratory for Smart Materials, School of Materials Science and Engineering, Harbin Institute of Technology (Shenzhen), Shenzhen 518055, China; Department of Mechanical and Energy Engineering, Southern University of Science and Technology, Shenzhen 518055, China*

Complete contact information is available at: https://pubs.acs.org/10.1021/acsnano.2c04596

### Author Contributions

†X.C. and Y.X. contributed equally to this work.


### Notes

The authors declare no competing financial interest.

## ACKNOWLEDGMENTS

The authors acknowledge helpful discussions with Igor Aronson and Darrell Velegol from Penn State University, Jiangxing Chen from Westlake University, and Mingcheng Yang from the Institute of Physics, CAS. Xi Chen, Yixin Peng, Chao Zhou, and Wei Wang are financially supported by the Science Technology and Innovation Program of Shenzhen (RCYX20210609103122038, JCYJ20190806144807401, and JCYJ20210324121408022) and the National Natural Science Foundation of China (11774075). Yankai Xu and Hepeng Zhang are supported by the National Natural Science Foundation of China (12074243 and 11774222).

## REFERENCES

(1) Deneke, V. E.; Di Talia, S. Chemical waves in cell and developmental biology. *J. Cell Biol.* **2018**, *217* (4), 1193–1204.

(2) Desai, R. C.; Kapral, R. *Dynamics of Self-organized and Self-assembled Structures*; Cambridge University Press: New York, 2009.
(3) Gelens, L.; Anderson, G. A.; Ferrell, J. E. Spatial trigger waves: positive feedback gets you a long way. *Mol. Biol. Cell* **2014**, *25* (22), 3486−3493.
(4) Tsuji, K.; Müller, S. C. *Spirals and Vortices In Culture, Nature, and Science*; Springer: Cham, 2019.
(5) Barr, L.; Dewey, M. M.; Berger, W. Propagation of Action Potentials and the Structure of the Nexus in Cardiac Muscle. *J. Gen. Physiol.* **1965**, *48* (5), 797−823.
(6) Hodgkin, A. L.; Huxley, A. F. A quantitative description of membrane current and its application to conduction and excitation in nerve. *J. Physiol.* **1952**, *117* (4), 500−544.
(7) Chang, J. B.; Ferrell, J. E., Jr Mitotic trigger waves and the spatial coordination of the Xenopus cell cycle. *Nature* **2013**, *500* (7464), 603−607.
(8) Speksnijder, J. E.; Sardet, C.; Jaffe, L. F. Periodic calcium waves cross ascidian eggs after fertilization. *Dev. Biol.* **1990**, *142* (1), 246−249.
(9) Stricker, S. A. Comparative Biology of Calcium Signaling during Fertilization and Egg Activation in Animals. *Dev. Biol.* **1999**, *211* (2), 157−176.
(10) Bers, D. M. Cardiac excitation-contraction coupling. *Nature* **2002**, *415* (6868), 198−205.
(11) Petrov, V.; Gaspar, V.; Masere, J.; Showalter, K. Controlling chaos in the Belousov—Zhabotinsky reaction. *Nature* **1993**, *361* (6409), 240−243.
(12) Showalter, K.; Epstein, I. R. From chemical systems to systems chemistry: Patterns in space and time. *Chaos* **2015**, *25* (9), 097613.
(13) Epstein, I. R.; Xu, B. Reaction-diffusion processes at the nano- and microscales. *Nat. Nanotechnol.* **2016**, *11* (4), 312−319.
(14) Tan, T. H.; Liu, J.; Miller, P. W.; Tekant, M.; Dunkel, J.; Fakhri, N. Topological turbulence in the membrane of a living cell. *Nat. Phys.* **2020**, *16* (6), 657−662.
(15) Jakubith, S.; Rotermund, H. H.; Engel, W.; von Oertzen, A.; Ertl, G. Spatiotemporal concentration patterns in a surface reaction: Propagating and standing waves, rotating spirals, and turbulence. *Phys. Rev. Lett.* **1990**, *65* (24), 3013−3016.
(16) Rotermund, H. H.; Engel, W.; Kordesch, M.; Ertl, G. Imaging of spatio-temporal pattern evolution during carbon monoxide oxidation on platinum. *Nature* **1990**, *343* (6256), 355−357.
(17) Kubota, R.; Makuta, M.; Suzuki, R.; Ichikawa, M.; Tanaka, M.; Hamachi, I. Force generation by a propagating wave of supramolecular nanofibers. *Nat. Commun.* **2020**, *11* (1), 3541.
(18) Grzybowski, B. A.; Huck, W. T. S. The nanotechnology of life-inspired systems. *Nat. Nanotechnol.* **2016**, *11* (7), 585−592.
(19) Wang, W.; Duan, W.; Ahmed, S.; Mallouk, T. E.; Sen, A. Small power: Autonomous nano- and micromotors propelled by self-generated gradients. *Nano Today* **2013**, *8* (5), 531−554.
(20) Soto, F.; Karshalev, E.; Zhang, F.; Esteban Fernandez de Avila, B.; Nourhani, A.; Wang, J. Smart Materials for Microrobots. *Chem. Rev.* **2022**, *122* (5), 5365−5403.
(21) Fernández-Medina, M.; Ramos-Docampo, M. A.; Hovorka, O.; Salgueiriño, V.; Städler, B. Recent Advances in Nano- and Micromotors. *Adv. Funct. Mater.* **2020**, *30* (12), 1908283.
(22) Chen, X.; Zhou, C.; Wang, W. Colloidal Motors 101: A Beginner's Guide to Colloidal Motor Research. *Chem-Asian J.* **2019**, *14* (14), 2388−2405.
(23) Colberg, P. H.; Reigh, S. Y.; Robertson, B.; Kapral, R. Chemistry in Motion: Tiny Synthetic Motors. *Acc. Chem. Res.* **2014**, *47* (12), 3504−3511.
(24) Wang, H.; Pumera, M. Coordinated behaviors of artificial micro/nanomachines: from mutual interactions to interactions with the environment. *Chem. Soc. Rev.* **2020**, *49* (10), 3211−3230.
(25) Huang, L.; Moran, J. L.; Wang, W. Designing chemical micromotors that communicate-A survey of experiments. *JCIS Open* **2021**, *2*, 100006.
(26) Jin, D.; Yuan, K.; Du, X.; Wang, Q.; Wang, S.; Zhang, L. Domino Reaction Encoded Heterogeneous Colloidal Microswarm with On-Demand Morphological Adaptability. *Adv. Mater.* **2021**, *33* (37), 2100070.
(27) Ibele, M. E.; Lammert, P. E.; Crespi, V. H.; Sen, A. Emergent, Collective Oscillations of Self-Mobile Particles and Patterned Surfaces under Redox Conditions. *ACS Nano* **2010**, *4* (8), 4845−4851.
(28) Zhou, C.; Chen, X.; Han, Z.; Wang, W. Photochemically Excited, Pulsating Janus Colloidal Motors of Tunable Dynamics. *ACS Nano* **2019**, *13* (4), 4064−4072.
(29) Chen, X.; Xu, Y.; Lou, K.; Zhou, C.; Peng, Y.; Zhang, H.; Wang, W. Unraveling the physiochemical nature of colloidal motion waves among silver colloids. *Sci. Adv.* **2022**, *8* (21), No. eabn9130.
(30) Zhou, C.; Suematsu, N. J.; Peng, Y.; Wang, Q.; Chen, X.; Gao, Y.; Wang, W. Coordinating an Ensemble of Chemical Micromotors via Spontaneous Synchronization. *ACS Nano* **2020**, *14* (5), 5360−5370.
(31) Altemose, A.; Sánchez-Farrán, M. A.; Duan, W.; Schulz, S.; Borhan, A.; Crespi, V. H.; Sen, A. Chemically controlled spatiotemporal oscillations of colloidal assemblies. *Angew. Chem., Int. Ed.* **2017**, *129* (27), 7925−7929.
(32) Schweizer, J.; Loose, M.; Bonny, M.; Kruse, K.; Mönch, I.; Schwille, P. Geometry sensing by self-organized protein patterns. *Proc. Natl. Acad. Sci. U. S. A.* **2012**, *109* (38), 15283−15288.
(33) Steinbock, O.; Kettunen, P.; Showalter, K. Anisotropy and Spiral Organizing Centers in Patterned Excitable Media. *Science* **1995**, *269* (5232), 1857−1860.
(34) Homma, K.; Masuda, T.; Akimoto, A. M.; Nagase, K.; Itoga, K.; Okano, T.; Yoshida, R. Fabrication of Micropatterned Self-Oscillating Polymer Brush for Direction Control of Chemical Waves. *Small* **2017**, *13* (21), 1700041.
(35) Bishop, K. J. M.; Grzybowski, B. A. Localized Chemical Wave Emission and Mode Switching in a Patterned Excitable Medium. *Phys. Rev. Lett.* **2006**, *97* (12), 128702.
(36) Masuda, T.; Akimoto, A. M.; Nagase, K.; Okano, T.; Yoshida, R. Artificial cilia as autonomous nanoactuators: Design of a gradient self-oscillating polymer brush with controlled unidirectional motion. *Sci. Adv.* **2016**, *2* (8), No. e1600902.
(37) Kuze, M.; Horisaka, M.; Suematsu, N. J.; Amemiya, T.; Steinbock, O.; Nakata, S. Chemical Wave Propagation in the Belousov-Zhabotinsky Reaction Controlled by Electrical Potential. *J. Phys. Chem. A* **2019**, *123* (23), 4853−4857.
(38) Das, N. P.; Dutta, S. Controlling three-dimensional vortices using multiple and moving external fields. *Phys. Rev. E* **2017**, *96* (2), 022206.
(39) Das, N. P.; Mahanta, D.; Dutta, S. Unpinning of scroll waves under the influence of a thermal gradient. *Phys. Rev. E* **2014**, *90* (2), 022916.
(40) Hwang, I.; Mukhopadhyay, R. D.; Dhasaiyan, P.; Choi, S.; Kim, S.-Y.; Ko, Y. H.; Baek, K.; Kim, K. Audible sound-controlled spatiotemporal patterns in out-of-equilibrium systems. *Nat. Chem.* **2020**, *12* (9), 808−813.
(41) Sakurai, T.; Mihaliuk, E.; Chirila, F.; Showalter, K. Design and Control of Wave Propagation Patterns in Excitable Media. *Science* **2002**, *296* (5575), 2009−2012.
(42) Epstein, I. R.; Gao, Q. Photo-Controlled Waves and Active Locomotion. *Chem.—Eur. J.* **2017**, *23* (47), 11181−11188.
(43) Totz, J. F.; Rode, J.; Tinsley, M. R.; Showalter, K.; Engel, H. Spiral wave chimera states in large populations of coupled chemical oscillators. *Nat. Phys.* **2018**, *14* (3), 282−285.
(44) Ren, L.; Wang, M.; Pan, C.; Gao, Q.; Liu, Y.; Epstein, I. R. Autonomous reciprocating migration of an active material. *Proc. Natl. Acad. Sci. U. S. A.* **2017**, *114* (33), 8704−8709.
(45) Zhang, S.; Shakiba, N.; Chen, Y.; Zhang, Y.; Tian, P.; Singh, J.; Chamberlain, M. D.; Satkauskas, M.; Flood, A. G.; Kherani, N. P.; Yu, S.; Zandstra, P. W.; Wheeler, A. R. Patterned Optoelectronic Tweezers: A New Scheme for Selecting, Moving, and Storing Dielectric Particles and Cells. *Small* **2018**, *14* (45), 1803342.
(46) Liang, Z.; Teal, D.; Fan, D. Light programmable micro/nanomotors with optically tunable in-phase electric polarization. *Nat. Commun.* **2019**, *10* (1), 5275.
(47) Arlt, J.; Martinez, V. A.; Dawson, A.; Pilizota, T.; Poon, W. C. K. Painting with light-powered bacteria. *Nat. Commun.* **2018**, *9* (1), 768.


https://doi.org/10.1021/acsnano.2c04596
*ACS Nano* 2022, 16, 12755−12766

(48) Palagi, S.; Mark, A. G.; Reigh, S. Y.; Melde, K.; Qiu, T.; Zeng, H.; Parmeggiani, C.; Martella, D.; Sanchez-Castillo, A.; Kapernaum, N.; Giesselmann, F.; Wiersma, D. S.; Lauga, E.; Fischer, P. Structured light enables biomimetic swimming and versatile locomotion of photo-responsive soft microrobots. *Nat. Mater.* **2016**, *15* (6), 647−653.
(49) Buskohl, P. R.; Vaia, R. A. Belousov-Zhabotinsky autonomic hydrogel composites: Regulating waves via asymmetry. *Sci. Adv.* **2016**, *2* (9), No. e1600813.
(50) Miller, P. W.; Stoop, N.; Dunkel, J. Geometry of Wave Propagation on Active Deformable Surfaces. *Phys. Rev. Lett.* **2018**, *120* (26), 268001.
(51) Yuan, P.; Kuksenok, O.; Gross, D. E.; Balazs, A. C.; Moore, J. S.; Nuzzo, R. G. UV patternable thin film chemistry for shape and functionally versatile self-oscillating gels. *Soft Matter* **2013**, *9* (4), 1231−1243.
(52) Rogers, J. M.; McCulloch, A. D. A collocation-Galerkin finite element model of cardiac action potential propagation. *IEEE Trans. Biomed. Eng.* **1994**, *41* (8), 743−757.
(53) Kapral, R.; Showalter, K. *Chemical waves and patterns*; Springer Science & Business Media: Dordrecht, 2012; Vol. *10*.
(54) Roth, B. Two-dimensional propagation in cardiac muscle. *Cardiac Electrophysiology, From Cell to Bedside*; 2000; 265−270.
(55) Chen, X.; Zhou, C.; Peng, Y.; Wang, Q.; Wang, W. Temporal Light Modulation of Photochemically Active, Oscillating Micromotors: Dark Pulses, Mode Switching, and Controlled Clustering. *ACS Appl. Mater. Interfaces* **2020**, *12* (10), 11843−11851.
(56) Tyson, J. J. *What Everyone Should Know About the Belousov-Zhabotinsky Reaction*; Springer Berlin Heidelberg, 1994; pp 569−587.
(57) Epstein, I. R.; Pojman, J. A. *An introduction to nonlinear chemical dynamics: oscillations, waves, patterns, and chaos*; Oxford University Press: New York, 1998.
(58) Lechleiter, J.; Girard, S.; Peralta, E.; Clapham, D. Spiral calcium wave propagation and annihilation in Xenopus laevis oocytes. *Science* **1991**, *252* (5002), 123−126.
(59) Glass, L.; Josephson, M. E. Resetting and Annihilation of Reentrant Abnormally Rapid Heartbeat. *Phys. Rev. Lett.* **1995**, *75* (10), 2059−2062.
(60) Kitahata, H.; Aihara, R.; Magome, N.; Yoshikawa, K. Convective and periodic motion driven by a chemical wave. *J. Chem. Phys.* **2002**, *116* (13), 5666−5672.
(61) Shiraki, Y.; Yoshida, R. Autonomous Intestine-Like Motion of Tubular Self-Oscillating Gel. *Angew. Chem., Int. Ed.* **2012**, *124* (25), 6216−6220.
(62) Epstein, I. R.; Gao, Q. Photo-Controlled Waves and Active Locomotion. *Chem.—Eur. J.* **2017**, *23* (47), 11181−11188.
(63) Petrov, V.; Ouyang, Q.; Swinney, H. L. Resonant pattern formation in achemical system. *Nature* **1997**, *388* (6643), 655−657.
(64) Bäuerle, T.; Löffler, R. C.; Bechinger, C. Formation of stable and responsive collective states in suspensions of active colloids. *Nat. Commun.* **2020**, *11* (1), 2547.
(65) Lozano, C.; Bechinger, C. Diffusing wave paradox of phototactic particles in traveling light pulses. *Nat. Commun.* **2019**, *10* (1), 2495.
(66) Wang, Q.; Zhou, C.; Huang, L.; Wang, W. Ballistic" Waves Among Chemically Oscillating Micromotors. *Chem. Commun.* **2021**, *57* (68), 8492−8495.
(67) Zhou, C.; Wang, Q.; Lv, X.; Wang, W. Non-oscillatory micromotors "learn" to oscillate on-the-fly from oscillating Ag micromotors. *Chem. Commun.* **2020**, *56* (48), 6499−6502.
(68) Wang, W.; Lv, X.; Moran, J. L.; Duan, S.; Zhou, C. A practical guide to active colloids: choosing synthetic model systems for soft matter physics research. *Soft Matter* **2020**, *16* (16), 3846−3868.
(69) O'Keeffe, K. P.; Hong, H.; Strogatz, S. H. Oscillators that sync and swarm. *Nat. Commun.* **2017**, *8* (1), 1504.
(70) Matsuda, Y.; Ikeda, K.; Ikura, Y.; Nishimori, H.; Suematsu, N. J. Dynamical Quorum Sensing in Non-Living Active Matter. *J. Phys. Soc. Jpn.* **2019**, *88* (9), 093002.
(71) Suematsu, N. J.; Nakata, S. Evolution of Self-Propelled Objects: From the Viewpoint of Nonlinear Science. *Chem.—Eur. J.* **2018**, *24* (24), 6308−6324.
(72) Gregor, T.; Fujimoto, K.; Masaki, N.; Sawai, S. The Onset of Collective Behavior in Social Amoebae. *Science* **2010**, *328* (5981), 1021−1025.
(73) Cui, R.-F.; Chen, Q.-H.; Chen, J.-X. Separation of nanoparticles via surfing on chemical wavefronts. *Nanoscale* **2020**, *12* (23), 12275−12280.
(74) Baudoin, M.; Thomas, J. L. Acoustic Tweezers for Particle and Fluid Micromanipulation. *Annu. Rev. Fluid Mech.* **2020**, *52* (1), 205−234.
(75) Jones, P. H.; Maragò, O. M.; Volpe, G. *Optical tweezers: Principles and applications*; Cambridge University Press: Cambridge, 2015.
(76) Sano, K.; Wang, X.; Sun, Z.; Aya, S.; Araoka, F.; Ebina, Y.; Sasaki, T.; Ishida, Y.; Aida, T. Propagating wave in a fluid by coherent motion of 2D colloids. *Nat. Commun.* **2021**, *12* (1), 6771.
(77) Chen, H.; Zhang, H.; Xu, T.; Yu, J. An Overview of Micronanoswarms for Biomedical Applications. *ACS Nano* **2021**, *15* (10), 15625−15644.
(78) Wang, W.; Zhou, C. A Journey of Nanomotors for Targeted Cancer Therapy: Principles, Challenges, and a Critical Review of the State-of-the-Art. *Adv. Healthcare Mater.* **2021**, *10* (2), 2001236.
(79) Cheng, Y.; Mou, F.; Yang, M.; Liu, S.; Xu, L.; Luo, M.; Guan, J. Long-range hydrodynamic communication among synthetic self-propelled micromotors. *Cell Rep. Phys. Sci.* **2022**, *3* (2), 100739.
(80) Chen, C.; Chang, X.; Teymourian, H.; Ramírez-Herrera, D. E.; Esteban-Fernández de Avila, B.; Lu, X.; Li, J.; He, S.; Fang, C.; Liang, Y.; Mou, F.; Guan, J.; Wang, J. Bioinspired Chemical Communication between Synthetic Nanomotors. *Angew. Chem., Int. Ed.* **2018**, *57* (1), 241−245.
(81) Oh, G.; Chung, E.; Yun, S. H. Optical fibers for high-resolution in vivo microendoscopic fluorescence imaging. *Opt. Fiber Technol.* **2013**, *19* (6, Part B), 760−771.
(82) Jiang, S.; Wu, X.; Rommelfanger, N. J.; Ou, Z.; Hong, G. Shedding light on neurons: optical approaches for neuromodulation. *Natl. Sci. Rev.* **2022**, DOI: 10.1093/nsr/nwac007




https://doi.org/10.1021/acsnano.2c04596
*ACS Nano* 2022, 16, 12755−12766